JOSEPHSON JUNCTION QUANTUM BITS AND THE QUANTUM MEASUREMENT PROCESS

Yuriy Makhlin
Institut für Theoretische Festkörperphysik, Universität Karlsruhe, D-76128 Karlsruhe, Germany
Landau Institute for Theoretical Physics, Kosygin St. 2, 117940 Moscow, Russia
makhlin@tfp.physik.uni-karlsruhe.de

Gerd Schön
Institut für Theoretische Festkörperphysik, Universität Karlsruhe, D-76128 Karlsruhe, Germany
schoen@tfp.physik.uni-karlsruhe.de

Alexander Shnirman
Department of Physics, University of Illinois at Urbana-Champaign, Urbana, IL 61801, USA
shnirman@london.physics.uiuc.edu

Abstract

Low-capacitance Josephson junctions can serve as physical realizations of quantum bits (qubits), with logical states differing by one Cooper-pair charge on an island. They combine the intrinsic coherence of the superconducting state with control of single-charge systems. The single- and two-bit operations required for quantum computation can be performed by applying sequences of voltage and current pulses. The phase coherence time is sufficiently long to allow a series of these steps. In addition to manipulations, the final state of the qubits has to be read out. This can be achieved by coupling them to a single-electron transistor. We analyze the quantum measurement process and provide a suitable set of system parameters.

1 Introduction

A quantum computer can solve certain problems which are untractable for classical computer in acceptable times [1, 2, 3, 4]. It is composed of a (large) number of coupled two-state quantum systems forming quantum bits (qubits). The computation is the quantum-coherent time evolution of the state of the system described by unitary transformations and controlled by the program. Elementary steps are (i) the preparation of the initial state of the qubits, (ii) single-bit operations (gates), i.e. unitary transformation of individual qubit states, triggered by a modification of the corresponding one-qubit Hamiltonian for some period of time, (iii) two-bit gates, which require controlled inter-qubit couplings, and (iv) the measurement of the final quantum state of the system. The phase coherence time has to be long enough to allow a large number of these coherent processes.

Several physical realizations of quantum information systems have been suggested. The best studied systems include trapped ions manipulated by laser irradiation, NMR on nuclear spins in molecules, and cavity QED. However, alternatives need to be explored, in particular those which are more easily embedded in an electronic circuit as well as scaled up to large numbers of qubits. From this point of view nano-electronic devices appear particularly promising [5, 6, 7, 8, 9, 10, 11]. Normal-metal single-electron devices are discussed in connection with classical digital applications and, in fact, constitute the ultimate electronic memory [12]. However, their use for quantum computation is ruled out, since, due to the large number of electron states involved, different tunneling processes are incoherent. Ultra-small quantum dots with discrete levels or spin degrees of freedom in nano-structured circuits are candidates [7, 8], but are difficult to fabricate in a controlled way. More promising are systems built from Josephson junctions, where the coherence of the superconducting state can be exploited. Quantum extension of elements based on a single-flux logic have been suggested [9], and attempts were made to observe coherent oscillations of flux quanta between degenerate states. Here we suggest to use low-capacitance Josephson junctions, where Cooper pairs tunnel coherently while Coulomb blockade effects allow the control of the total charge. If biased near degeneracy these junctions constitute qubits with two logical states differing by one Cooper-pair charge on an island.

A simple design of Josephson junction qubits and their coupling (reviewed below) has been suggested in Ref. [5]. Single-bit operations can be performed by controlling gate voltages applied to individual junctions, while two-bit gates can be implemented by tuning two selected qubits to resonance. The dephasing time has been estimated to be large compared to elementary operation times. To read out the quantum state a dissipative normal-metal single-electron transistor should be coupled to the qubit [13]. The small number of junctions and control voltages of the simple design simplify an experimental realization. Drawbacks are the continuing time evolution of the states also dur-

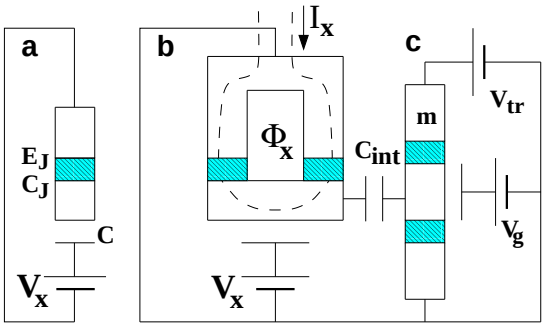

Figure 1: (a) Josephson junction qubit; (b) qubit with SQUID-controlled coupling; (c) measuring SET.

ing idle periods, which necessitates a high precision of the time control, as well as intrinsic errors introduced by nonvanishing two-bit couplings even if the qubits are out of resonance. An improved design, still based on nano-scale Josephson junction technology, brings us closer to the ideal case [6]. The crucial step is the replacement of the Josephson junctions by SQUIDs which can be controlled by external magnetic fluxes. This allows us to switch the Josephson couplings on and off. It substantially reduces the requirements on the time control and provides a complete control of two-bit couplings.

The fabrication of the circuits described below is possible with present-day technology. In fact, it has been already demonstrated experimentally that in such systems eigenstates are superpositions of (macroscopically) different charge states [11, 14, 15]. Moreover, very recently coherent oscillations between two charge states have been observed in a Josephson qubit, which was initially prepared in a superposition of eigenstates [16]. This was the first observation of macroscopic quantum coherence effects (MQC[17]). This demonstration of the first functioning nano-electronic qubit is a basis for further developments in the field. One of next goals would be the demonstration of controlled manipulations of coupled qubits.

2 Josephson qubits and logic gates

2.1 The simplest design of the qubit

The simplest Josephson junction qubit is shown in Fig. 1a. It consists of a small superconducting island connected by a tunnel junction, with capacitance $C_{\rm J}$ and Josephson coupling energy $E_{\rm J}$, to a superconducting electrode. An external voltage source, $V_{\rm x}$, is connected to the system via a gate capacitance C. We assume that the superconducting energy gap Δ is the largest energy in the problem, larger even than the single-electron charging energy to be discussed below. In this case quasi-particle tunneling is suppressed at low temperatures, and a situation can be achieved where no quasiparticle excitations exist on the island. Thus, in the following, we will consider the situation where only Cooper pairs tunnel in the superconducting junction. This system is described by the Hamiltonian

$$\sum_n E_{\rm ch}(n)|n\rangle\langle n| - \frac{1}{2}E_{\rm J}\left(|n\rangle\langle n+1| + |n+1\rangle\langle n|\right). \quad (1)$$

Here, n is the number of extra Cooper pair charges on the island (relative to some neutral reference state). The second term in (1) is usually presented as $E_{\rm J}\cos\Theta$, where the phase difference Θ is conjugated of the charge n. The charging energy of the superconducting island, $E_{\rm ch}(n) \equiv 4E_C(n-n_{\rm qb})^2$, is characterized by the scale $E_C \equiv e^2/2(C+C_{\rm J})$, while the dimensionless gate charge, $n_{\rm qb} \equiv CV_{\rm x}/2e$, acts as a control field. We consider systems where E_C is much larger than the Josephson coupling energy, $E_C \gg E_{\rm J}$. In this regime a convenient basis is formed by the charge states, parameterized by the number of Cooper pairs n on the island.

For most values of $n_{\rm qb}$ the energy levels are dominated by the charging part of the Hamiltonian. However, when $n_{\rm qb}$ is approximately half-integer and the charging energies of two adjacent states are close to each other, the Josephson tunneling mixes them strongly (see Fig. 2). We concentrate on the voltage interval near a degeneracy point of two charge states, say $n=0$ and $n=1$. For the parameters chosen, further charge states can be ignored, and the system (1) reduces to a two-state model, with Hamiltonian which can be written in spin-$\frac{1}{2}$ notation in terms of Pauli spin matrices $\vec{\sigma} = \sigma_x, \sigma_y, \sigma_z$ as

$$H = \frac{1}{2}\Delta E_{\rm ch}(V_{\rm qb})\sigma_z - \frac{1}{2}E_{\rm J}\sigma_x \ . \quad (2)$$

The charge states $n=0$ and 1 correspond to the basis states $|\downarrow\rangle \equiv \binom{0}{1}$ and $|\uparrow\rangle \equiv \binom{1}{0}$, respectively. The difference in the charging energy $\Delta E_{\rm ch}(V_{\rm x}) \equiv E_{\rm ch}(n=1) - E_{\rm ch}(n=0) = 4E_C(1-2n_{\rm qb})$, equivalent to the field in z-direction, is controlled by the gate voltage.

2.2 Qubit with SQUID-controlled coupling

The crucial step towards the ideal design is to have a tunable Josephson coupling. This is achieved in the circuit shown in Fig. 1b, where each Josephson junction is replaced by a dc-SQUID threaded by the magnetic flux. The SQUID is biased by an external flux $\Phi_{\rm x}$, which is coupled into the system through an inductor loop. If the self-inductance of the SQUID loop is low [18], the SQUID-controlled qubit is described by a Hamiltonian of the form (2), but with the coupling strength

$$E_{\rm J}(\Phi_{\rm x}) = 2E_{\rm J}^0\cos\left(\pi\frac{\Phi_{\rm x}}{\Phi_0}\right) \quad (3)$$

and effective junction capacitance $C_{\rm J} = 2C_{\rm J}^0$. I.e., the effective Josephson coupling $E_{\rm J}(\Phi_{\rm x})$ is tunable by varying the external flux $\Phi_{\rm x}$ by amounts of the order of the flux quantum $\Phi_0 = hc/2e$ between $2E_{\rm J}^0$ and zero. For convenience we can further rewrite the Hamiltonian as

$$H = \frac{1}{2}\Delta E\left(\cos\eta\ \sigma_z - \sin\eta\ \sigma_x\right) \ . \quad (4)$$

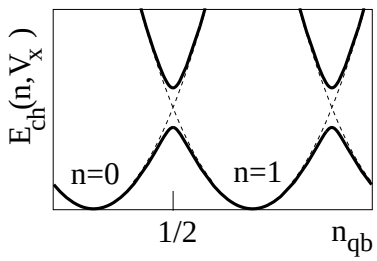

Figure 2: The charging energy of the superconducting electron box is shown (parabolas) as a function of the gate charge $n_{\rm qb}$ for different numbers of extra Cooper pairs n on the island. Near degeneracy points the weaker Josephson coupling energy mixes the charge states and modifies the energy of the eigenstates (solid line). In this regime the system effectively reduces to a two-state quantum system.

The mixing angle $\eta(V_{\rm x},\Phi_{\rm x}) = \tan^{-1}[E_{\rm J}/\Delta E_{\rm ch}(V_{\rm qb})]$ determines the direction of the effective magnetic field in the xz-plane, and the energy splitting between the eigenstates is $\Delta E = E_{\rm J}/\sin\eta$. At the degeneracy point, $\eta = \pi/2$, it reduces to $E_{\rm J}$. For some chosen value of $n_{\rm qb}$ the eigenstates of the Hamiltonian are

$$\begin{aligned} & \cos\frac{\eta}{2}\,|{\downarrow}\rangle + \sin\frac{\eta}{2}\,|{\uparrow}\rangle \\ - \quad & \sin\frac{\eta}{2}\,|{\downarrow}\rangle + \cos\frac{\eta}{2}\,|{\uparrow}\rangle \quad . \end{aligned}$$

2.3 Single-qubit logic gates

We choose the idle regime of the system (between the operations) as the regime with $\Delta E_{\rm ch} = 0$, $E_{\rm J} = 0$, i.e. with no evolution of the quantum state, and $|0\rangle = |{\uparrow}\rangle$ and $|1\rangle = |{\downarrow}\rangle$ as the logical states. By changing the gate voltage and/or magnetic flux we can perform the required one-bit operations (logic gates). For example, switching the flux suddenly away from $\Phi_0/2$ for a time Δt and then switching back produces a rotation in spin space,

$$U_{1-\rm bit}(\Delta t) = \exp\left(i\alpha\sigma_x\right) = \begin{pmatrix} \cos\alpha & i\sin\alpha \\ i\sin\alpha & \cos\alpha \end{pmatrix},$$

where $\alpha = E_{\rm J}(\Phi_{\rm x})\Delta t/2\hbar$. Depending on the value of Δt, a spin flip can be produced, or, starting from $|0\rangle$, a superposition of states with any chosen weights can be reached. Similarly a temporary change of the voltage by a small amount away from the degeneracy point produces the energy difference between the logical states and hence produces a relative phase shift, in this case by an angle $\beta = \Delta E_{\rm ch}\Delta t/2\hbar$.

This spin rotations and phase shifts are elementary one-qubit operations. They provide a universal set of single-qubit gates, that is any single-qubit unitary transformation can be performed as a sequence of these elementary ones. Typical time spans of single-qubit logic gates are determined by corresponding energy scales and are of order $\hbar/E_{\rm J}$, $\hbar/\Delta E_{\rm ch}$, for x- and z-rotations, respectively. The energies $\Delta E_{\rm ch}(V_{\rm x})$ and $E_{\rm J}(\Phi_{\rm x})$ can be optimized such that the duration of the manipulations $\tau_{\rm op}$ is long enough to simplify time control and short enough to speed up the computation.

2.4 Controlled inter-qubit coupling

The SQUID-controlled Josephson junctions allow us also to switch the two-qubit interaction individually for each pair of qubits. The simplest implementation of the coupling is to connect all N qubits in parallel to each other to an inductor L (Fig. 3). The frequency of the LC-mode in the resulting circuit is $\omega_{LC} = (NC_{\rm qb}L)^{-1/2}$, where the capacitance of a qubit in the external circuit is $C_{\rm qb} = C_{\rm J}C/(C_{\rm J}+C)$. If it is large, $\hbar\omega_{LC} \gg E_{\rm J}, \Delta E_{\rm ch}, k_{\rm B}T$ the fast oscillations produce an effective coupling of the qubit dynamics [5]

$$\mathcal{H}_{\rm int} = -\sum_{i<j} \frac{E_{\rm J}(\Phi_{{\rm x}i})E_{\rm J}(\Phi_{{\rm x}j})}{E_L}\hat\sigma_y^i\hat\sigma_y^j, \qquad (5)$$

where $E_L = \frac{\Phi_0^2}{\pi^2 L}\left(\frac{C_{\rm J}}{C_{\rm qb}}\right)^2$, and $E_{\rm J}^i = E_{\rm J}(\Phi_{{\rm x}i})$ are the effective Josephson energies of the qubits, controlled by the external fluxes. The coupling energy (5) can be understood as the magnetic energy of the current in the inductor, where the current is the sum of the contributions from the qubits with non-zero Josephson coupling, $I^i \propto E_{\rm J}^i\hat\sigma_y^i$.

Using this interaction we can perform all gate operations. In the idle state all Josephson couplings are turned off and the interaction Hamiltonian (5) is zero. The same is true during a one-qubit operation, as long as we perform one such operation at a time: i.e. only one $E_{\rm J}^i \neq 0$. To perform a two-qubit operation with any given pair of qubits, say 1 and 2, $E_{\rm J}^1$ and $E_{\rm J}^2$ are switched on simultaneously, yielding the total Hamiltonian

$$\mathcal{H} = -\frac{E_{\rm J}^1}{2}\hat\sigma_x^1 - \frac{E_{\rm J}^2}{2}\hat\sigma_x^2 + \frac{E_{\rm J}^1E_{\rm J}^2}{E_L}\hat\sigma_y^1\hat\sigma_y^2\,. \qquad (6)$$

Typical time spans of two-bit operations are of the order $\hbar E_L/E_{\rm J}^2$. These operations, combined with the one-bit operations discussed above, provide a universal set of gates sufficient for quantum computation.

3 Dissipation and dephasing

The idealized picture above discussed should be extended to account for dissipation mechanisms which lead to dephasing of the qubit's state. Below we estimate the effect of fluctuations in the external circuit which are modeled by finite resistances of the voltage and current sources. Internal dissipation in the Josephson junctions is a weaker effect. Another important source of dephasing are the fluctuations of the background charge. This $1/f$-noise is difficult to estimate analytically but it should be relatively weak at the frequencies of the qubit operation.

The qubit is manipulated through external voltage and current sources. They are part of a dissipative circuit, characterized by an effective frequency-dependent impedance $Z(\omega)$. In the considered frequency range the

typical dimensions of the external circuit are much larger than the wavelength of light, and from the point of the qubit the circuit can be considered as a waveguide with a purely resistive impedance R_V of the order of the vacuum impedance ($\sim 100\Omega$). Accordingly, the applied voltages and fluxes are fluctuating. This introduces random $\hat{\sigma}_z$- and $\hat{\sigma}_x$-components in the qubit Hamiltonian which induces incoherent transitions between qubit levels and fluctuations of their eigenenergies. As a result, off-diagonal elements of the qubit density matrix decay on a certain time scale while diagonal elements tend to their thermal equilibrium values. Following Refs.[19, 20] we can estimate the corresponding decoherence rates as follows:

$$\Gamma_V^{\rm d} = \gamma_V \frac{\Delta E}{\hbar} \frac{\sin^2\eta}{\tanh(\Delta E/2k_{\rm B}T)}\,, \qquad (7)$$

$$\Gamma_V^{\rm od} = \gamma_V \frac{\Delta E}{\hbar}\left[\frac{\sin^2\eta}{2\tanh\left(\frac{\Delta E}{2k_{\rm B}T}\right)} + \frac{\cos^2\eta}{\Delta E/2k_{\rm B}T}\right]. \qquad (8)$$

The mixing angle $\eta(\Phi_{\rm x}, V_{\rm g})$ and the energy splitting ΔE were defined in Section 2.2. The parameter

$$\gamma_V = 4\pi \frac{R_V}{R_{\rm K}}\left(\frac{C_{\rm qb}}{C_{\rm J}}\right)^2$$

determines the strength of the fluctuations. The dephasing is weak if the ratio of R_V and the quantum resistance $R_{\rm K} = h/e^2 \approx 26{\rm k}\Omega$ is small. Furthermore, a small gate capacitance $C \approx C_{\rm qb} \ll C_{\rm J}$ helps decoupling the qubit from the environment. If both are optimized, the phase coherence time is much longer than typical operation times of order $\hbar/\Delta E$.

The circuit of the current source with resistance R_I, which couples the flux $\Phi_{\rm x}$ to the SQUID by the mutual inductance M, also introduces fluctuations and dephases the qubit dynamics. The decoherence rates are given by expressions similar as (7) and (8) with prefactor

$$\gamma_I = \pi^3 \frac{R_K}{R_I}\frac{E_{\rm J}}{\Phi_0^2/M}\sin^2\left(\frac{\pi\Phi_{\rm x}}{\Phi_0}\right)\,. \qquad (9)$$

The dephasing due to fluctuations in the current source is slow if its resistance is high and the coupling to the qubit via a mutual inductance M is weak.

The η- and T-dependence of different contributions to the dephasing rates (7) and (8), and similar for the influence of the current fluctuations, can be understood from the following physical picture: We can think of a qubit as a spin-1/2 particle in the magnetic field $\vec{H} = \frac{1}{2}\Delta E(\cos\eta\hat{z} - \sin\eta\hat{x})$. Voltage and current fluctuations described above induce random fields in z- and x-directions, that is, fluctuating fields both along perpendicular to $\vec{H}$. The frequency-dependence of the rms fluctuations is given by the Johnson-Nyquist formula, $\omega\coth(\hbar\omega/2k_{\rm B}T)$. The zero-frequency Fourier component of longitudinal random fields induces fluctuations of eigenenergies (last term in (8)), while the $\Delta E/\hbar$ resonance of the transverse fluctuations induces incoherent transitions between the eigenstates (first terms in (7) and (8)).

Here the dephasing rates were estimated for the simplest case of a resistive external circuit. An improved design, with narrow-band filters between the external circuit and the superconducting box, which filter out low-frequency noise but let through high-frequency driving pulses, can significantly enhance the coherence time.

4 Energy and time scales

So far we concentrated on the two lowest energy states of the qubit. But the qubit is a macroscopic solid-state system and has a number of excited states. These states should stay empty during the computation. To formulate relevant constraints on system parameters let us estimate the gap between the two lowest states and the rest of the energy spectrum.

First of all, charge states with the number of Cooper pairs different from n or $n+1$ are separated from the qubit states by a gap of the order $3E_C$ in the vicinity of degeneracy points. Odd-parity states, with an unpaired electron on the island, are gapped by an amount larger or equal to $\Delta - E_C$. Apart from that, higher-energy levels of flux oscillations in the SQUID or of LC-oscillations in the LC-circuit which couples the qubits can be excited. They are separated by corresponding oscillation energy quanta, $\hbar\omega_\Phi$ and $\hbar\omega_{LC}$. Finally, the single-electron transistor used to measure the quantum state of the qubit is also characterized by some excitation energy.

For the higher states to have no effect upon the computation: (i) They should not be occupied in the initial state of the qubit. To achieve this the temperature should be much smaller than the gap: $T \ll E_C, \Delta - E_C, \hbar\omega_{LC}, \hbar\omega_\Phi$. (ii) They should not be excited during the qubit evolution. Since the qubit evolves on a frequency scale determined by its Hamiltonian, that is at frequencies of order[1] $E_{\rm J}/\hbar$ and $\Delta E_{\rm ch}/\hbar$, we require $E_{\rm J}, \Delta E_{\rm ch} \ll E_C, \Delta - E_C, \hbar\omega_{LC}, \hbar\omega_\Phi$. (iii) An additional time scale of the qubit evolution is set by the switching time, $\tau_{\rm sw}$, of the external voltages and fluxes between different operations. The switching should be slow enough in order not to excite the higher states: $\hbar/\tau_{\rm sw} \ll E_C, \Delta - E_C, \hbar\omega_{LC}, \hbar\omega_\Phi$.

As for the ratio of the switching time, $\tau_{\rm sw}$, and the qubit evolution times, $\hbar/E_{\rm J}$, $\hbar/\Delta E_{\rm ch}$, there is no fundamental limitation on it. However, there are two limits which are convenient for an explicit description (a) the switching is much faster than the period of the qubit oscillations ("instantaneous" switching); (b) the switching is much slower ("adiabatic" switching). In the latter case additional resonance ac-driving pulses should be applied after the switching in order to perform logic gates.

[1] $E_{\rm J}$ and $\Delta E_{\rm ch}$ are determined by the external voltages and fluxes. Their typical values during an operation enter in the following estimate.

5 Read-out: quantum measurement

The read-out of the state of a qubit requires a quantum measurement process. This can be accomplished by coupling a normal-state single-electron transistor (SET) capacitively to the qubit (see Fig. 4). The charging energy of the SET is of order $E_{\rm SET}$, its tunneling resistance is $R_{\rm SET}$, and the capacitive coupling is described an an energy $E_{\rm int}$. The important aspect is that during the quantum manipulations the SET is kept deeply in the Coulomb blockade regime. Hence no dissipative currents flow in the system, and dephasing effects due to the transistor are minimized. The SET only adds to the total capacitance. When the SET is driven out of equilibrium it quickly dephases the qubit, while the tunnel current through the SET depends on the charge configurations of the qubit. The description of this quantum measurement process, which has been performed in Ref. [13] by an explicit analysis of the time-evolution of the density matrix of the coupled system, shows that the process is characterized by three time scales introduced below.

We reduce the density matrix in two different ways in order to obtain dual descriptions of the measurement. The first procedure is to study the reduced 2×2 density matrix $\hat\rho$ of the qubit itself. If at the beginning of the measurement the qubit was in a superposition of logical states, $a\,|0\rangle + b\,|1\rangle$, then the density matrix was $\rho_{00} = |a|^2$, $\rho_{11} = |b|^2$, $\rho_{01} = \rho_{10}^* = ab^*$. The questions are how fast the off-diagonal elements of $\hat\rho$ vanish due to dephasing by the SET, and how fast the diagonal elements change their original values (mixing due to transitions between the two states).

When the transistor is turned on, random tunneling processes destroy the phase coherence of the qubit within a short time

$$\tau_\varphi^* \approx \hbar \frac{R_{\rm K}}{R_{\rm SET}} \frac{E_{\rm SET}}{E_{\rm int}^2} \,,$$

that is the off-diagonal matrix-elements vanish. On a very long "mixing" time scale,

$$t_{\rm mix} \approx \hbar \frac{\Delta E^3}{E_{\rm int}^2 E_{\rm J}^2} \left(\frac{R_{\rm SET}}{R_{\rm K}} \frac{\Delta E}{E_{\rm SET}} + \frac{R_{\rm K}}{R_{\rm SET}} \frac{E_{\rm SET}}{\Delta E} \right) \,,$$

transitions between the qubit's levels erase the information about the initial state of the qubit.

The second procedure is to evaluate the probability distribution, $P(m,t)$, of the number of electrons m, which nave tunneled through the SET during time t. At $t = 0$ no electrons have tunneled, so $P(m,0) = \delta_{m,0}$. Then the current starts flowing and this peak begins to shift towards positive m, and, at the same time, it widens due to shot noise. Since two states of the qubit correspond to different conductivities, one may hope that after some time the peak splits into two. If after sufficient separation of the two peaks their weights are still close to $|a|^2$ and $|b|^2$, a good quantum measurement has been performed. Unfortunately, the mixing destroys this idealized picture. After a long time the two peaks transform into a broad plateau.

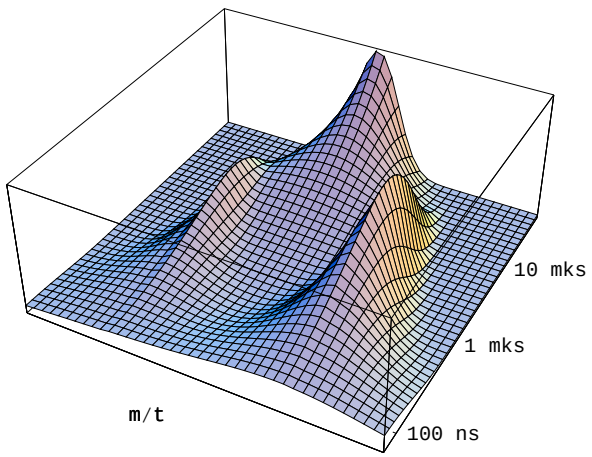

Figure 3: $P(m/t,t)$, the probability that m electrons tunneled during time t, for initial amplitudes of the qubit's state $a = \sqrt{0.75}$ and $b = \sqrt{0.25}$. The double-peak structure, which allows the measurement, is observed only in the range between $t_{\rm meas}$ and $t_{\rm mix}$. For convenience, we use the log-scale for the time axis. The most probable values of m (peaks) scale linearly with time.

One should find an optimum time for the measurement, so that, on one hand, the two peaks have separated and, on the other hand, the mixing has not yet happened. The analysis shows that the measurement is accomplished after a longer time, of order

$$t_{\rm meas} \approx \hbar \frac{R_{\rm SET}}{R_{\rm K}} \frac{E_{\rm SET}}{E_{\rm int}^2} \,,$$

when the signal resolves the different quantum states. In the range of the validity of our approach the measurement time exceeds the dephasing time, $t_{\rm meas} \gg \tau_\varphi^*$, consistent with the fact that a quantum measurement implies complete dephasing of the quantum state. For a good quantum measurement we also need that $t_{\rm mix} \gg t_{\rm meas}$, and this regime can be realized for technologically available system parameters. The typical outlook of $P(m,t)$ in this regime is shown in Fig.3.

6 Discussion

To demonstrate that the constraints on the circuit parameters can be met by available technology, we suggest a suitable set:

(i) We choose junctions with capacitance $C_{\rm J} = 3 \cdot 10^{-16}$F, corresponding to a charging energy (in temperature units) $E_C \approx 3$K, and a smaller gate capacitance $C = 2{\cdot}10^{-17}$F to reduce the coupling to the environment. The superconducting gap has to be slightly larger $\Delta > E_C$. Thus at a temperature of order $T = 50$mK the initial thermalization is assured. We further choose $E_{\rm J}^0 = 50$mK, i.e. the time scale of one-qubit operations is $\tau_{\rm op}^{(1)} = \hbar/E_{\rm J} \approx 7 \cdot 10^{-11}$s. For these parameters fluctuations in the gate voltage circuit, with resistance $R_V \approx 50\Omega$, limit the coherence time to $(\Gamma_V \tau_{\rm op}^{(1)})^{-1} \approx 10^4$ operations.

(ii) With the parameters $L_\Phi = 0.1$nH, $M = 1$nH and

$R_I = 10^2$–$10^6\Omega$, the flux circuit has a weak dephasing effect compared to voltage fluctuations.
(iii) To assure fast two-bit operations we choose $L \approx 3\mu$H. Then $(\Gamma_V \tau_{\rm op}^{(2)})^{-1} \approx 500$ two-bit gates can be performed before the phase coherence is lost. With these parameters the number of qubits in the circuit can be chosen in the range of 10 to 50, of course at the expense of shorter coherence times which are reduced proportional to $1/N$.

The system presented here does not permit parallel operations on different qubits, which is an essential element of many powerful quantum algorithms. It can be achieved in principle by a more advanced design, making use, e.g., of further tunable SQUIDs decoupling different parts of the circuit. Such modifications, as well as further progress of nano-technology, will provide longer coherence times and allow scaling to larger numbers of qubits. We note, however, that many aspects of quantum information processing can initially be tested on simple circuits as proposed here.

7 Experiment

Recently key features of the system described above have been demonstrated experimentally. A group from NEC, Tsukuba [16] observed coherent oscillations of the system between two different charge states. In the experiment the system was kept at a voltage away from degeneracy and had time to relax to the ground charge state. Then it was driven for a finite time to the degeneracy point, where Josephson tunneling ($H_x \sim E_{\rm J}/2$) induces coherent oscillations between two charge states with a period determined by $E_{\rm J}$. The probability to find the system excited to another charge state at the end of the pulse exhibits periodic oscillations as a function of the time span of the driving voltage pulse. This probability was probed by an additional junction. This measurement setup is simpler than the one discussed in Section 5 and is easier to fabricate, but it has the disadvantage of introducing a source of dephasing [16]. A number of parameters (the initial voltage before the pulse as well as a flux-controlled $E_{\rm J}$) were varied, and the period of oscillations followed the theoretical predictions. This experiment demonstrates the quantum mechanical nature of the system at low temperatures and is the first experimental realization of a solid-state quantum bit. Furthermore, recent developments in SET-electrometer design [21] should allow faster measurement procedures. With these advances the realization of small quantum information systems of several qubits and the investigation of their quantum mechanical features should be possible in the near future.

8 Acknowledgments

We thank T. Beth, M. Devoret, D. P. DiVincenzo, E. Knill, K. K. Likharev, and J. E. Mooij for stimulating discussions.

9 References

[1] Lloyd, S., Science **261**, 1589 (1993).

[2] Bennett, C.H., Physics Today **48** (10), 24 (1995).

[3] DiVincenzo, D.P., Science **269**, 255 (1995).

[4] Barenco, A., Contemp. Phys. **37**, 375 (1996).

[5] Shnirman, A., Schön, G., and Hermon, Z., Phys. Rev. Lett. **79**, 2371 (1997).

[6] Makhlin, Yu., Schön, G., and Shnirman, A., Nature, **398**, 305 (1999).

[7] Loss, D., DiVincenzo, D.P., Phys. Rev. A **57**, 120 (1998).

[8] Kane, B.E., Nature **393**, 133 (1998)

[9] Mooij, J.E. et al., "Josephson persistent current qubit", prepint

[10] Averin, D.V., Solid State Commun. **105**, 659 (1998).

[11] Bouchiat, V., Joyez, P., Esteve, D., and Devoret, M., Physica Scripta **T76**, 165 (1998).

[12] Korotkov, A.N., Chen, R.H., and Likharev, K.K., J. Appl. Phys. **78**, 2520 (1995).

[13] Shnirman, A., and Schön, G., Phys. Rev. B **57**, 15400 (1998).

[14] Maassen v.d. Brink, A., Schön, G., and Geerligs, L.J., Phys. Rev. Lett. **67**, 3030 (1991).

[15] Nakamura, Y., Chen, C.D., and Tsai, J.S., Phys. Rev. Lett. **79**, 2328 (1997).

[16] Nakamura, Y., Pashkin, Yu.A., and Tsai, J.S., Nature **398**, 786 (1999).

[17] Leggett, A.J., in: "Chance and Matter". Elsevier, 1987.

[18] see, e.g., Tinkham, M. Introduction to Superconductivity. McGraw-Hill, New York, 1996.

[19] Leggett, A.J. et al., Rev. Mod. Phys. **59**, 1 (1987).

[20] Weiss, U. Quantum dissipative systems. World Scientific, Singapore, 1993.

[21] Schoelkopf, R.J. et al., Science **280**, 1238 (1998).